

Molecular motors and the forces they exert[☆]

Michael E. Fisher, Anatoly B. Kolomeisky

Institute for Physical Science and Technology, University of Maryland, College Park, MD 20742, USA

Abstract

The stochastic driving force that is exerted by a single molecular motor (e.g., a kinesin, or myosin protein molecule) moving on a periodic molecular track (such as a microtubule, actin filament, etc.) is discussed from a general theoretical viewpoint open to experimental test. An elementary but fundamental “barometric” relation for the driving force is introduced that (i) applies to a range of kinetic and stochastic models of catalytic motor proteins, (ii) is consistent with more elaborate expressions that entail further, explicit assumptions for the representation of externally applied loads and, (iii) sufficiently close to thermal equilibrium, satisfies an Einstein-type relation in terms of the observable velocity and dispersion, or diffusion coefficient, of the (load-free) motor protein on its track. Even in the simplest two-state kinetic models, the predicted velocity-vs.-load plots (that are observationally accessible) exhibit a variety of contrasting shapes that can include *nonmonotonic* behavior. Previously suggested bounds on the driving force are shown to be inapplicable in general by considering discrete jump models which feature waiting-time distributions. Some comparisons with experiment are sketched. ©1999 Elsevier Science B.V. All rights reserved.

1. Introduction

Molecular motors are individual protein molecules that are ultimately responsible for essentially all “active” biological motion including internal material transport. Important examples are myosin, kinesin, dynein, and RNA polymerase [2–6]. These molecules will move along appropriate, periodically structured, linearly polarized molecular tracks, such as actin filaments, microtubules, and DNA strands. They perform tasks vital to the life of the organism — muscle contraction, bacterial motion, cell division, intracellular transport, and genomic transcription [2–6]. Understanding how the various molecular motors operate represents a significant scientific challenge.

[☆] This article represents an expanded and significantly extended version of a more concise paper by the same authors — Ref. [1: PNAS 96 (1999) 6597–6602] — that, however, is closely followed in places. Some notational simplifications are also introduced here.

The hydrolysis of adenosine triphosphate (ATP), with the release of adenosine diphosphate (ADP) and inorganic phosphate (P_i), is known to be the power source for many motor proteins. In the simplest picture — which, nonetheless, seems rather accurate in many cases — a single molecule of ATP diffuses in solution, encounters a motor protein attached to a molecular track, and lodges in an active site on the motor. The motor protein then catalyzes the decomposition of the bound ATP molecule into $ADP + P_i$, releasing, in the process, a significant quantity of energy: that engenders a major conformational change in the motor protein resulting, after final discharge of the reaction products, in the net movement of the motor along the molecular track in a “forward” direction by one discrete step, say of size d . Under a sufficiently high ambient concentration of ATP in the solution the catalytic process then repeats with another ATP molecule, and the motor protein takes a further step forward. Of course, thermal fluctuations must introduce statistical features. Clearly, then, an activated motor may well be in a dynamical or, better, a stochastic steady state but it *cannot* be in full thermal equilibrium.

In recent years striking *in vitro* experiments have actually observed individual motor protein molecules moving along fixed tracks under controlled external loads [7–13]¹ in accordance with this scenario. Such motility studies, employing optical traps, force clamps, etc., have stimulated enhanced theoretical work aimed at understanding the mechanisms by which a biological motor functions.

Now, from a broad theoretical perspective one may regard a molecular motor simply as a microscopic object that moves (predominantly in one direction) along a directed or “polar” one-dimensional periodic lattice, i.e., the molecular track [1–13] in accordance with some “laws of motion” — presumably of basically stochastic character. Furthermore, the motor may be subject to an external force F , which might vary spatially (or, even with time, t). The questions of interest are, then: “What *driving force*, say f , can the motor exert? What mean velocity, V , will it display? How will the velocity achieved depend on the load, F ?” And: “Since the displacement, say x , along the track is stochastic, what *dispersion*,

$$D \approx [\langle x^2(t) \rangle - \langle x(t) \rangle^2] / 2t \quad (1)$$

(or effective diffusion constant), will the motor display with respect to its mean position, $\langle x(t) \rangle \approx Vt$, at time t (under steady-state conditions)?”

To provide a more concrete conception, let us mention that for the much studied motor protein kinesin, which moves on microtubules [3–11,13], the single-step size is $d \simeq 8.2$ nm, while velocities up to $V \lesssim 800$ nm/s, and forces as large as, roughly, $f \simeq 6$ piconewtons (pN) are observed. The detailed data display dispersions of magnitude $D \simeq 1500$ nm²/s [8,13]. Concentrations of ATP in the range $1\mu M \lesssim [ATP] \lesssim 10$ mM have been studied [13]. But note, by contrast, that RNA polymerase (which

¹ The recent article by Visscher et al. [13], appearing after [1], provides extensive data, especially regarding the dependence on ATP concentration, which, however, is not reflected in our discussion in Section 7 here. We plan to present an analysis in the future [28].

Table 1
Forces related to a molecular motor

Force	Notation and relations	Eq.
Maximum driving force	$f_{\max} = \Delta G_0/d > f$	(13)
Einstein scale	$f_E = k_B TV/D < f$	(15)
Gravitational force	$f_G = mg$	(20)
Barometric force	$f_B = k_B T \kappa \cong f$	(17, 21)
Stalling force	$f_S = k_B T \epsilon / \theta d \stackrel{?}{=} f$	(31)
Load and stalling load	$F, F_S, \eta = F/F_S$	(32)

is powered by nucleoside triphosphates that release pyrophosphate, PP_i) displays velocities of 30–40 nucleotides/s and can generate forces up to $f \simeq 25$ pN [12].

The aim of the work reported here [1] is *not* to treat detailed (or realistic) models of various motor proteins that embody the quantitative features just sketched. Rather, it is to construct a general theoretical framework² in which to address, in particular, *how* the driving force, f , should be calculated for a broad class of molecular motor models; to relate the driving force to the velocity and to the dispersion, insofar as that is, in fact, appropriate; and to discuss the way in which the external load force, F , should be incorporated in a model. A sense of where the reader will be taken may be gained by perusing Table 1: this lists the various forces (and force scales) we will be led to consider and, for reference, includes the corresponding defining equations presented below.

To prepare the ground, we outline, in the following section, a general class of discrete-state stochastic/kinetic models which embody basic features of a multitude of more specific treatments found in the literature. Following a previous lead [15], we show how a striking analysis by Derrida [16] for arbitrary periodic one-dimensional random walks (an extension of which we plan to publish), provides an exact and *explicit* analytical tool for the task in hand. (see also the appendix here and, for a more restricted scheme, the appendix of Ref. [8].) In the subsequent section we consider the maximum driving force and an “Einstein force scale”, that is related to the dispersion D (see Table 1). Our main result, presented in Section 4, is the proposal of a general “barometric” expression for the force, f , which, we believe, is the most appropriate candidate for predicting the driving force from a specific model. Then, in Section 5, we consider the introduction of external loads, demonstrating how it is essential to allow for *load distribution factors* which determine the response of the internal transitions in the motor protein to imposed stresses. With this formulation in hand, we investigate the velocity vs. load plots that may be derived: the allowed shapes, even for the simplest ($N=2$)-state models, present a surprising diversity: see Figs. 3–4 below. To check the general theory against reality, a brief discussion of experiments on kinesin is presented on the basis of the ($N=2$)-state models in Section 7: significant features of the theory are confirmed, although further detailed experimental tests are

² Aspects of our treatment appear, although in a considerably less general setting, in work by Hong Qian [14].

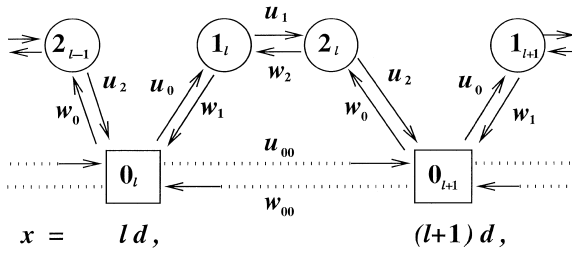


Fig. 1. Schematic representation of the sequential kinetic scheme (2) for describing a motor protein in the case $N=3$. The squares denote resting states free of any power supplying molecule, the circles correspond to “active” internal states. The initial forward rate, u_0 , may be expected to be proportional to the concentration of ATP or other power source. The dotted lines represent the possibility of “spontaneous” forward and backward processes *not* dependent on an explicit molecular power source (such as ATP): see text.

most certainly desirable and simulations could be useful. Finally, Section 8 exposes an artificial limitation of the simplest kinetic descriptions by introducing discrete jump models which have waiting-time distributions [17]. (It is for such models, in particular, that we have extended Derrida’s analysis [16].) Our main conclusions are summarized briefly in Section 9.

2. Molecular motor models

Traditionally, and in simplest terms one studies catalytic reactions, as exemplified by motor proteins, via kinetic chemical descriptions: see, for example [14,18] and references therein. Recently, in addition to various more detailed schemes [12,13,19–21], so-called “isothermal ratchet” models (that postulate pairs of periodic ‘saw-tooth’ potentials) have been proposed to account for the mechanics: see the reviews [22,23] and, e.g. [14,24,25].

Now, a common feature of most approaches is that a motor protein molecule is associated with a labeled site l ($=0, \pm 1, \pm 2, \dots$) on the track (or linear lattice) and can be pictured as residing in one of N essentially discrete states j , which may be *free of* or *bound to* a power-source molecule, say, ATP and its various hydrolysis products. We will take $j = 0$ to label the free state and $j = 1, 2, \dots, N - 1$ to label the various bound states. Consider, as an illustration, a kinesin molecule, K, on a microtubule, M: the ($N = 4$) states identified might be: $M \cdot K$, $M \cdot K \cdot \text{ATP}$, $M \cdot K \cdot \text{ADP} \cdot \text{P}_i$, and $M \cdot K \cdot \text{ADP}$ [9,18]. Transition rates between these states can be introduced via the sequential kinetic scheme (see Fig. 1).

$$\begin{array}{ccccccc}
 u_0 & u_1 & & u_{N-2} & & u_{N-1} & \\
 0_l \rightleftharpoons 1_l \rightleftharpoons \cdots \rightleftharpoons (N-1)_l \rightleftharpoons 0_{l+1}, & & & & & & (2) \\
 w_1 & w_2 & & w_{N-1} & & w_0 &
 \end{array}$$

where the subscripts indicate that the states j are associated with successive sites, l and $l + 1$, on the track spaced at distances $\Delta x = x_{l+1} - x_l = d$: this defines the *step*

size d , as introduced above. Of course, states $j_l, j_{l+1}, \dots, j_{l+n}$ differ physically only in their spatial displacements $d, 2d, \dots, nd$, along the track. By the same token, the rates u_j and w_j are independent of l (or $x = ld$);³ however, in the subsequent developments it will prove useful to allow for spatially varying rates $u_j(l)$ and $w_j(l)$. The “laws of motion” are now given by the standard rate equations

$$\frac{\partial}{\partial t} P_j(l; t) = u_{j-1}(l) P_{j-1}(l; t) + w_{j+1}(l) P_{j+1}(l; t) - [u_j(l) + w_j(l)] P_j(l; t), \quad (3)$$

for $j = 0, 1, \dots, N - 1$, where $P_j(l; t)$ is the probability of finding the motor in state j at site l at time t , and, in order to maintain the underlying periodicity we make the identifications

$$P_{-1}(l; t) \equiv P_{N-1}(l - 1; t), \quad P_N(l; t) \equiv P_0(l + 1; t),$$

$$u_{-1}(l) = u_{N-1}(l - 1) \quad \text{and} \quad w_N(l) = w_0(l). \quad (4)$$

One may, conveniently for many purposes, suppose that the motor starts from the origin $l = x = 0$ in a free state so that $P_j(l; 0) = \delta_{j0} \delta_{l0}$.

To properly represent physicochemical reality (that is, microscopic reversibility) *none* of the forward rates, u_j , or backward rates w_j may strictly vanish even though in reality some, such as the last reverse rate, $w_N \equiv w_0$ might be extremely small [12,15,18]. On the other hand, if, as indeed observed in the presence of free ATP (or other power source), the motor moves under no external load to the right (increasing x), the transition rates *cannot* (all) satisfy the usual conditions of detailed balance that would characterize thermal equilibrium if the scheme (2) were regarded as a set of chemical reactions (near equilibrium) between effective species j_l [22].

It is of practical significance to notice that the first forward transition in (2), in which, say, a free ATP molecule initially binds to the motor protein, may be envisaged chemically as a second-order rate process, e.g., $M \cdot K + \text{ATP} \rightleftharpoons M \cdot K \cdot \text{ATP}$. Then, for sufficiently low concentrations of ATP one can conclude that $u_0 = k_0[\text{ATP}]$, where $k_0(T)$ is a concentration-independent rate constant. This, in turn, can lead to Michaelis–Menten-type rate-vs.-concentration relations [7,13] of the overall form

$$\mathcal{R} \simeq \mathcal{R}_{\max}[\text{ATP}]/([\text{ATP}] + K_M), \quad (5)$$

where \mathcal{R} is some rate of interest (that might be the motor velocity, V). The Michaelis–Menten constant, K_M , in fact sets the concentration at which $\mathcal{R} = \frac{1}{2} \mathcal{R}_{\max}$.

However, as illustrated in Fig. 1 for an ($N=3$)-state system, one might also contemplate a small “spontaneous” or first-order background rate, $u_{00} > 0$, that exists even in the absence of ATP. A corresponding backward rate w_{00} , should then also be included. Except in the trivial $N=1$ case (where u_{00} can simply be included in u_0 and w_{00} in w_0) this changes the linear nature of the kinetic scheme (2): however, while many of our explicit algebraic expressions (for $V(F)$, D , etc.) will then hold only if $u_{00} = w_{00} = 0$

³Note that in [1] the forward rates denoted here by u_0, \dots, u_{N-1} , were called u_1, \dots, u_N , respectively, while the backward rate w_0 here (“out of the state $j = 0$ ”) was called w_N . Beyond these changes which, in particular, simplify Eq. (3) and other expressions, we follow the notations of [1].

(as we shall assume henceforth), all the general conceptual principles of our discussion will still apply.

Now, within statistical physics, the kinetic scheme in Eqs. (2)–(4) represents a one-dimensional hopping process of a particle on a periodic but, in general, *asymmetric* lattice. After initial transients, the particle will move with steady (mean) velocity V , and diffuse [with respect to the mean position, $\langle x \rangle = Vt$, at time t : see (1)] with a diffusion constant D [16,17,26,27]. Complicated, but exact and explicit equations for V and D in terms of the rate constants u_j and w_j have been obtained for all N by Derrida [16]: for reference, these are exhibited in our notation in the appendix. To describe the transient behavior more labor is required: however, for the case $N=2$ explicit integral expressions can be found for the probabilities $P_j(l;t)$ introduced in (3): see [15] and, more generally, the appendix of [1].

One immediately observes from Eq. (A.1) that a dimensionless, overall rate factor, that appears rather naturally, is given by the product

$$\Gamma = \prod_{j=0}^{N-1} \left(\frac{u_j}{w_j} \right) \equiv e^\varepsilon. \quad (6)$$

This will play a central role in our discussion. Note, indeed, that viewing (2) as a standard set of chemical reactions and requiring detailed balance would impose $\Gamma \equiv 1$ (or $\varepsilon = 0$) whereas $\Gamma > 1$ (or $\varepsilon > 0$) is evidently needed for a positive velocity V . (One might recall, however, [15] that as regards the *full* chemistry, the complex of motor protein plus track may be regarded simply as catalyzing the hydrolysis of ATP (or other power source): the reaction rates for the corresponding *overall* isothermal process may then be expected to satisfy detailed balance.)

The simplest or “minimal” physical models for a motor protein must clearly have $N = 2$. As mentioned, one can then calculate analytically not only the steady-state behavior but also the full transient responses. In Ref. [15] only the special (limiting) case with $w_0 = 0$ was treated; but as will be seen below, this limit can be misleading and so the general $N = 2$ results were presented in [1]. Here we will use only the velocity and diffusion constant for $N = 2$: these can conveniently be written in the forms

$$V = \frac{(u_0 u_1 - w_0 w_1) d}{u_0 + u_1 + w_0 + w_1} \equiv (\Gamma - 1) \omega d, \quad (7)$$

$$D = \frac{1}{2} [\Gamma + 1 - 2(\Gamma - 1)^2 \omega / \sigma] \omega d^2, \quad (8)$$

where $\Gamma = u_0 u_1 / w_0 w_1$, as in (6), and we have introduced the associated overall rates

$$\sigma = u_0 + u_1 + w_0 + w_1, \quad \omega = w_0 w_1 / \sigma. \quad (9)$$

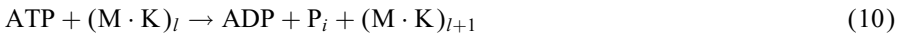
As already illustrated in Fig. 1, one can, of course, envisage more complicated schemes than (2) that include various branches, internal loops, parallel pathways, detachment, etc. Thus, for example, a backwards reaction directly from, say, state j_l^\dagger to the original unbound or free state 0_l could account for “futile” ATP hydrolysis,

i.e., “consumption” of an ATP molecule but without any forward motion of the motor [19]. Note, however, that within the $N = 2$ models (which enforce $j^{\dagger} = 1$) this phenomenon may be described simply by including the futile-hydrolysis parallel reaction rate in the backward rate w_1 . In all cases, however, there will be a well-defined (zero-load) steady-state velocity V and a diffusion constant D (both independent of the particular states, j); and these are susceptible to estimation by simulation even should their explicit mathematical expressions be intractable (although for general u_{00} , w_{00} (see Fig. 1) and for branches and detachments, etc., closed-form results can also be obtained [28]). Furthermore, in real systems both V , as often demonstrated [7,9–13], and D [8,13] are susceptible to experimental measurement as explained.

Now there arises an obvious but crucial question, namely: “What (mean) driving force, f , will such a general motor protein model exert as it moves along its track?” That is the principal issue we have to address.

3. Maximum and Einstein force scales

For concreteness, let us suppose the molecular motor is kinesin and, thus, is powered by ATP. If the hydrolysis



was, hypothetically, performed in vacuo at low temperatures, so that all reactants and products were in their (quantum mechanical) ground states, a definite energy ΔE_0 would be released by the reaction. This would then be available as mechanical energy and, so, could move the motor through the step size $\Delta x = d$ from state 0_l to 0_{l+1} exerting an effective force $f_0 = \Delta E_0/d$. In practise, however, the catalytic hydrolysis process, *in vitro* or *in vivo*, takes place in solution and essentially isobarically and isothermally, at ambient pressures and temperatures, say (p_0, T_0) . It is then more reasonable to regard the reaction as releasing a free energy, say ΔG_f , which, physically, accounts for the presence of solvent, of thermal fluctuations, etc.

If one were considering an overall bulk chemical reaction



with (relatively low) concentrations $[A], [B], \dots$, one would compute the free energy released via

$$\Delta G = \Delta G_0 + RT \ln([C][D][E]/[A][B]) , \quad (12)$$

where ΔG_0 is referred to standard conditions, which, to sufficient accuracy, we may take as (p_0, T_0) : see, e.g. [29,30]. Then, comparing (10) and (11), it is tempting to make identifications $A = \text{ATP}$, $B = (\text{M} \cdot \text{K})_l$, etc.: accepting those and the value ΔG_0 of about 0.50×10^{-19} J, corresponding to 7.3 kcal/M or $12 k_B T$ at typical *in vitro* temperatures, T [4], one obtains $\Delta G \simeq 20 k_B T$ by using reasonable estimates for

typical cellular concentrations $[ATP], \dots$, etc.⁴ However, that is not, we believe, the appropriate way to identify ΔG_f . Rather, in understanding the operation of a molecular motor, one should be concerned with the microscopically local release of free energy by ATP adsorbed on the motor-protein-track complex. The appropriate concentrations to use in (12) are then to be determined essentially only by the stoichiometry of the reaction. Thus, in addition to the obvious concentration ratio $[E]/[B] = [(M \cdot K)_{l+1}]/[(M \cdot K)_l] = 1$, we should, in (12), also take $[C][D]/[A] = [ADP][P_i]/[ATP] = 1$. This leads directly to $\Delta G = \Delta G_0$; consequently, we accept ΔG_0 as a most reasonable estimate of ΔG_f , the locally released free energy.

If all the free energy $\Delta G_f = \Delta G_0$ could be converted into mechanical energy and move the motor protein through the step size, d , the force exerted would be

$$f_{\max} = \Delta G_0/d. \quad (13)$$

Accepting that one molecule of ATP (or other power source) is sufficient to translocate the motor protein by one step [8], this expression clearly represents the maximal driving force that can be exerted. For a kinesin moving on a microtubule [7–13] with $d \simeq 8.2$ nm [10,13] it yields $f_{\max} \simeq 6.2$ pN. Then, if f is the driving force actually realized, the *efficiency* of a molecular motor protein may sensibly be defined by $\mathcal{E} = f/f_{\max}$.

To gain further insight, consider a small (“mesoscopic”) particle with “instantaneous” position $x(t)$ and velocity $v(t)$ that undergoes one-dimensional Brownian motion in a fixed, slowly varying external potential, $\Phi(x)$. Under a constant external force, $F = -(d\Phi/dx)$, the particle will diffuse with a diffusion constant which, for long times, t , satisfies the relation (1) in which, now $\langle \cdot \rangle$ denotes an equilibrium, statistical mechanical average [26,27,31,32]. In addition, the particle experiences an (effective) *frictional force*, $f_E = \zeta v(t)$, where ζ is a friction coefficient determined by the environment [26,27,31,32]. In a steady state, the friction balances the external force, F , leading to a drift motion, $\langle x(t) \rangle \approx Vt$, with mean velocity given by $V = F/\zeta = f_E/\zeta$. Now, by definition, Brownian motion takes place within *full thermal equilibrium*: that fact dictates [26,27,31,32] the Einstein relation

$$\zeta = k_B T/D \quad (14)$$

which, in turn, implies the result

$$f_E = k_B TV/D \quad (15)$$

for what we will call the *Einstein force scale* — the second entry in Table 1.⁵

In the present context this is an appealing formula since it determines a force in terms *only* of the velocity, V , and the dispersion, D . As discussed, these are directly predictable by a motor-protein model — see, e.g. (7)–(9) above; likewise, V and

⁴ We acknowledge stimulating remarks conveyed in correspondence with Hong Qian.

⁵ Note that Svoboda et al. [8] choose to characterize fluctuations in the movement of the motor in terms of a “randomness parameter” r which, in our notation, is given simply by $r = 2D/Vd$. Thus the Einstein scale can also be expressed as $f_E = 2k_B T/dr$.

D are observable in an experiment or a simulation. However, because an activated molecular motor is *not* a Brownian particle and *cannot*, as explained, be described by thermal equilibrium alone, there are really no grounds for expecting f_E to be related to the proper driving force, f . Nevertheless, we will show that in a certain limit such a Brownian motion “mimic” of an activated motor protein does provide an adequate prediction for f . Indeed, Ref. [15] accepted the identification $f = f_E$ without discussion and used relation (15) to estimate driving forces for the restricted ($w_1=0$) $N=2$ models. The values of f so obtained were not unreasonable in comparison with experimental data [15]: see further discussion below.

It is also worth pointing out that Ref. [33] (see also [19]) invokes an Einstein relation in an analysis of observations of “protein friction”. However, this is a rather different context in which many “blocked” motor proteins (that cannot hydrolyze ATP) are attached to a substrate and a rigid microtubule diffuses, apparently freely, close-by in the medium above. Quantitative arguments [19,33] explain the large frictional slowdown seen — relative to an appropriate Einstein-relation estimate using the solvent viscosity — as due to weak protein binding on to and unbinding off the microtubule.

4. Barometric formulation for the driving force

Although the identification of the motor driving force f with the Einstein scale, f_E , is unjustified, it is certainly desirable to have a soundly based, general expression for f which, like f_E , does *not* entail any intrinsic modifications or extensions of the motor model or of the associated physicochemical picture beyond the specified rate constants. To that end, let us consider the placement of an “impassable block” or *barrier* on the molecular track, say, between sites L and $L+1$ ($\gg 1$) or at distance $x=X=Ld$ from the origin $x=0$ (fixed, as we have already supposed, by where the motor starts): see Fig. 2.

Such a barrier may be realized theoretically by decreeing that all states j_l for $l \geq L+1$ are inaccessible. This may be achieved simply by setting one of the local forward rate constants, say, $u_j(l=L)$, equal to zero so the motor can never pass beyond the state J_l . No other rate constants need be modified: thus essentially no change of the basic molecular model is entailed. Nevertheless, if further nearby rate constants are changed, it will have no consequences for our main conclusions. One might actually want to do this to take cognizance of some aspects of a real barrier that might be attached to a molecular track in an experimental set-up.

It is intuitively clear that running a (real or model) molecular motor up to such a barrier will lead — provided it does not detach from the track or “freeze” irreversibly, as might happen in practice [7,11] — to some stationary probability distribution, as sketched in Fig. 2. It is convenient to write this distribution as

$$P_j(l; t \rightarrow \infty) = P_j^\infty(L-l) \quad (16)$$

with $z = (L-l)d = X-x$ so that z measures the distance back from the barrier: see Fig. 2. On very general theoretical grounds one should expect this distribution to

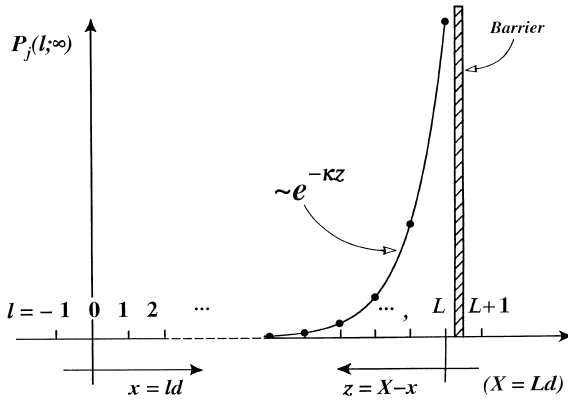


Fig. 2. Depiction of a barrier placed on a molecular motor track between sites L and $L + 1$, and of the exponentially decaying stationary probability distribution that builds up when a motor is run up against the barrier: see relation (17) and the accompanying text.

decay exponentially with increasing z except for possible deviations close to the barrier. Consequently, we can write

$$P_j^\infty(z/d) \approx A_j e^{-\kappa z}, \quad (z \gg d), \tag{17}$$

where the (positive) decay constant κ should, in principle, be experimentally measurable (although this may be difficult if κd is large). The amplitude ratios A_j/A_0 ($j = 0, 1, \dots, N - 1$) must depend on the various rate ratios, u_i/w_i , while A_0 may be determined simply by normalization of the overall probability distribution.

To justify this surmise for the kinetic equations (3) (although it is of much more general validity), note that the mean flow between adjacent states $(N - 1)_{l-1}$ and 0_l and between $(j - 1)_l$ and j_l [for $j = 1, 2, \dots, (N - 1)$] must vanish for a stationary distribution (with no net current flow). Balancing local forward and backward rates thus yields

$$\begin{aligned} u_{N-1}(l-1)P_{N-1}^\infty(L-l+1) &= w_0(l)P_0^\infty(L-l), \\ u_{j-1}(l)P_{j-1}^\infty(L-l) &= w_j(l)P_j^\infty(L-l), \end{aligned} \tag{18}$$

for $j = 1, 2, \dots, (N - 1)$. Starting from an initial nonzero value $P_j^\infty(0)$, one can then recursively determine $P_{j-1}^\infty(0), P_{j-2}^\infty(0), \dots, P_0^\infty(0), P_{N-1}^\infty(1), P_{N-2}^\infty(1), \dots$. By induction, this leads directly to the exponential decay (17) [since the $u_j(l)$, and $w_j(l)$ become independent of l for, say, $l < L - l_0$ where l_0 is some small fixed integer representing the extent of influence of the barrier on the transition rates]. Most crucially one finds, recalling the definition (6), that the decay constant is simply given by

$$\kappa = (\ln \Gamma)/d = \varepsilon/d. \tag{19}$$

Now, to interpret these results in terms of some effective driving force, consider a dilute gas of molecules of mass m moving in a gravitational field that acts “downwards”

along the vertical or z -axis. Each molecule then has a weight $f_G = mg$; in addition, the equilibrium density distribution is given by [34]

$$\rho(z) = \rho(0)e^{-mgz/k_B T} = \rho(0)\exp[-(f_G/k_B T)z], \quad (20)$$

where $\rho(0)$ is the density at the level $z=0$. (Any deviations arising close to the “lower” wall (at $z \simeq 0$) due to molecular size, structure, etc., have, of course, been neglected.) Comparing this well-known barometric formula with the analogous barrier distribution (17) leads us to identify the driving force f of the molecular motor with f_G and, thence, with

$$f_B = k_B T(\ln \Gamma)/d = k_B T\varepsilon/d. \quad (21)$$

This is one of our principal results: the subscript B serves merely to indicate the barometric analogy underlying our identification. It is significant to note that, by comparison with (13) for f_{\max} , we may expect

$$\varepsilon \lesssim \Delta G_0/k_B T \quad (22)$$

for any real molecular motor.

4.1. Barometric vs. Einstein scale

Before studying this result in relation to extensions of the simple kinetic scheme (2) that are needed to describe a motor functioning under external loads, let us compare f_B with f_E . To start, let us suppose the molecular motor operates close to equilibrium in the sense that $\varepsilon = \ln \Gamma$ is small. (Recall that detailed balance, in equilibrium, would require $\Gamma = 1$ and $\varepsilon = 0$.) Then, on expanding in $\varepsilon = 0$ at fixed ω/σ , Eqs. (6)–(9) and (21) yield

$$f_B/f_E = 1 + [\frac{1}{12} - (\omega/\sigma)]\varepsilon^2 - \frac{1}{2}(\omega/\sigma)\varepsilon^3 + \dots \quad (23)$$

for $N = 2$. Evidently, the coefficient of ε vanishes identically! Furthermore, one finds $0 < \omega/\sigma \leq \frac{1}{16}$ so that the coefficient of ε^2 is small, lying between $\frac{1}{48}$ and $\frac{1}{12}$. Consequently, and as might well have been anticipated, the Einstein scale approximates the barometric result very well when the motor operates sufficiently close to equilibrium. Indeed, for $\Gamma < 10$, calculations show that f_B can exceed f_E by no more than 44%. Furthermore, the series in (23) truncated at $O(\varepsilon^2)$ proves reasonably accurate up to $\varepsilon \simeq 5$ ($\Gamma \simeq 150$) where one has $1.473 < f_B/f_E < 2.535$; beyond that one can establish the effective bounds,

$$\frac{1}{4}\varepsilon < f_B/f_E \lesssim \frac{1}{2}\varepsilon. \quad (24)$$

These specific results are limited to $N = 2$; however, the vanishing of the $O(\varepsilon)$ term in (23) is independent of N . Indeed, the basic symmetry of the kinetic scheme (2) under the forward–backward transition rate interchanges: $w_0 \Leftrightarrow u_{N-1}$ and $w_j \Leftrightarrow u_{j-1}$ ($j = 1, \dots, N-1$), and $\varepsilon \Leftrightarrow -\varepsilon$, leads to $\Gamma \Leftrightarrow 1/\Gamma$, $V \Leftrightarrow -V$, while D remains invariant: consequently,⁶ the ratio f_B/f_E is essentially an even function of ε . (It is

⁶We are indebted to B. Widom for a remark on this point.

only because we chose, in (23), to expand at fixed ω , which is not an invariant under the rate exchange, that an $O(\varepsilon^3)$ term appears).

By the same token, we expect f_B always to rise steadily above f_E when ε increases. Indeed, on recalling (16) for Γ , one observes from (21) that f_B is unbounded above and so, with an injudicious assignment of rate constants, it may even exceed f_{\max} , as given in (13)! Conversely, one may show from (7), (8) and (15), that f_E , the Einstein force scale, is bounded above by $4k_B T/d$ for $N=2$ [15]. However, we will demonstrate in Section 8 that this bound on f_E is rather artificial and does *not* apply for models that account in a more direct fashion for the discreteness of the hydrolysis of ATP (or other power source molecules).

5. The effects of a load

In a typical experiment on motor proteins [7–11], optical tweezers are used to carry a silica bead coated with a few molecules of the motor protein up to a molecular-track filament secured on a glass surface. Then a single motor binds to the track and, in the presence of a power source, spontaneously starts to move, exerting a force against the opposing load, F , as it pulls the bead away from the center of the optical trap. In leading approximation, the external force F is a linear function of the displacement of the motor from the trap center, and the constant of proportionality can be measured. Thus the trap and bead work like a calibrated spring acting on the molecular motor. (Alternatively [13], with the aid of appropriate feedback controls, a constant force can be applied.) To represent such experiments, the load-free scheme embodied in (2) must, clearly, be extended.

To this end, suppose the motor moves on the track in a slowly varying external potential, $\Phi(x)$, so that in translocating from site l to $l+1$ (say, in the free state $j=0$), additional mechanical work

$$W_l \equiv \Delta\Phi(x=ld) = \Phi(x+d) - \Phi(x), \quad (25)$$

must be done (relative to the load-free situation). Of course, this corresponds to imposition of a local external force, $F(x) = \Delta\Phi(x)/d$ (or $F_l = W_l/d$), directed negatively. For an (ideal) optical trap of spring constant K we may take

$$\Phi(x) = \frac{1}{2}Kx^2, \quad F(x) = K(x + \frac{1}{2}d). \quad (26)$$

Our analysis will not, however, depend on any specific form for $\Phi(x)$ although, for conceptual simplicity, we will suppose $F(x)$ increases with x .

In such a situation the motor should, in effect, compress the spring and, as t increases, attain a stationary distribution, say $P_0^S(l)$, where, for simplicity, we focus only on the (free) states 0_l . This distribution should peak at some l_S , corresponding to a mean (or most probable) compression of the spring by a displacement $x_S = l_S d$. Then the measured “stalling force” [in the harmonic situation (26)] would be $f_S = Kx_S$.

Now it is evident physically that under any local load, $F(x)$, the transition rates, $u_j(l)$ and $w_j(l)$, must change. If, as traditional, one views the chemical transitions

between successive states, j and $j + 1$, as proceeding in quasiequilibrium over various free energy barriers [19], one expects (in leading approximation) the rates to change exponentially with $F(x)d/k_B T$. But a crucial question now arises, namely, “How should the exponential loading factors be distributed among the various reaction processes, $j \rightleftharpoons (j + 1)$, occurring “inside” the motor protein ?” This is far from obvious: indeed, the way in which the load is shared should, clearly, be of considerable interest in understanding the motor mechanism at a more detailed microscopic level.

To avoid prejudice, therefore, we advance the *quasiequilibrium hypothesis* that under a local load, F , acting “at” site l , the individual transition rates change in accord with

$$u_j \Rightarrow u_j^{(F)} = u_j^{(0)} e^{-\theta_j^+ Fd/k_B T}, \quad w_j \Rightarrow w_j^{(F)} = w_j^{(0)} e^{+\theta_j^- Fd/k_B T} . \quad (27)$$

The *load distribution factors*, θ_j^+ and θ_j^- , introduced here need not be of uniform sign: but we certainly expect the overall factor

$$\theta = \sum_{j=0}^{N-1} (\theta_j^+ + \theta_j^-) , \quad (28)$$

to be positive, since that simply implies that the load force acts to oppose motion. Indeed, should the motor undergo diffusion in thermal equilibrium when *not* activated by ATP [as suggested in Fig. 1 and in the discussion following (5)], detailed-balance considerations would dictate $\theta = 1$. As a *supplement* to our quasiequilibrium hypothesis this value of θ is also plausible for an activated motor that operates not too far from equilibrium.

Notice, however, that an individual *negative* θ_j^+ or θ_j^- simply means that the corresponding forward rate, u_j , is *enhanced*, or the reverse rate, w_j , is *diminished* by the internal molecular strain induced in the motor by the load. There are no good reasons for excluding such possibilities. Indeed, it is not difficult to imagine concrete mechanisms that would lead to such effects: for example, suppose an adsorption site on the protein were covered by a “lid” that was pulled open by imposing a load against a spring that otherwise held it closed.

If we accept the hypothesis (27), we can find the stationary “spring-compression” distribution $P_0^S(l)$ with the aid of the rate-balance the relations (18), simply by replacing $P_j^\infty(L - l)$ by $P_j^S(l)$, and the rates u_j and w_j in accord with (27). By iterating on j the relations (18) lead to

$$P_0^S(l + 1) = \frac{u_{N-1}(l)}{w_0(l)} P_{N-1}^S(l) = \frac{u_{N-1}(l)}{w_0(l)} \frac{u_{N-2}(l)}{w_{N-1}(l)} P_{N-2}^S(l) = \dots . \quad (29)$$

The most probable motor location, l_S , then follows by equating $P_0^S(l)$ and $P_0^S(l + 1)$, which yields the condition

$$\Gamma^{(F)}(l) \equiv \prod_{j=0}^{N-1} [u_j^{(F)}(l)/w_j^{(F)}(l)] = \Gamma^{(0)} e^{-\theta F(x)d/k_B T} = 1 . \quad (30)$$

Solving this determines $x_S = l_S d$ and hence, by identifying $F(x_S)$ with f_S , the measured spring or *stalling force*, yields our second principal result, namely,

$$f_S = k_B T (\ln \Gamma) / \theta d = k_B T \varepsilon / \theta d, \quad (31)$$

see Table 1. Here, of course, we have identified the zero-load rate factor, $\Gamma^{(0)}$, with the original rate factor Γ defined in (6) in terms of the *unmodified* transition rates u_j and w_j ($j = 0, 1, \dots, N - 1$).

It is striking that this expression for the stalling force — which rests on the quasiequilibrium hypothesis (27) that is needed to extend the original kinetic model — agrees *precisely* with the barometric expression (21) for f_B , provided one accepts the natural, near-equilibrium evaluation $\theta = 1$. We regard this overall consistency as strengthening both approaches.

6. Velocity versus load

The extended rate constants $u_j^{(F)}$ and $w_j^{(F)}$ introduced in hypothesis (27) also serve to provide a relation for $V(F)$, the motor velocity, as a function of a steady load force, F , and, equally, for the load-dependent diffusion constant $D(F)$: see [13] for recent experimental results. For arbitrary N one may appeal to (A1) which shows, as expected, that the stalling load, F_S , which brings $V(F)$ to zero, agrees with (31), i.e., $F_S = f_S$. To write an explicit result for $N = 2$ in an illuminating form, we introduce the reduced force and modified load distribution factors

$$\eta = F/F_S \quad \text{and} \quad \Delta_j^\pm = \frac{1}{2} - (\theta_j^\pm / \theta). \quad (32)$$

Then by combining (7), (27) and (31) we can construct the expression

$$\frac{V(F)}{V(0)} = \frac{\sigma \sinh[\frac{1}{2}\varepsilon(1 - \eta)] / \sinh(\frac{1}{2}\varepsilon)}{u_0 e^{-\Delta_1^+ \varepsilon \eta} + u_1 e^{-\Delta_0^+ \varepsilon \eta} + w_0 e^{\Delta_1^- \varepsilon \eta} + w_1 e^{\Delta_0^- \varepsilon \eta}}, \quad (33)$$

where, naturally, $V(0)$ is simply the no-load result stated in (7), so that the right-hand side must reduce to unity when $\eta = 0$ (while it vanishes when $\eta \rightarrow 1$). For convenience, we recall that $\varepsilon = \ln(u_0 u_1 / w_0 w_1)$.

Now for ε small (say, $\lesssim 2$), so that the motor is operating not too far from equilibrium, one has

$$V(F) \approx V(0)(1 - \eta)/(1 + c\varepsilon\eta). \quad (34)$$

This represents a *hyperbolic* force law which will be *concave* or *convex* depending on the sign, + or -, of c : see the illustrative examples in Fig. 3.⁷ Concave plots, like (b) in Fig. 3, are characteristic of experiments on animal muscles: see, e.g. [2, Fig. 2.19].

⁷Note, that in the caption for Fig. 1 of [1] the data for the plot (c) — the same plot as reproduced here — contains a misprint: the value of ε should read 9.2 (as specified in the caption here).

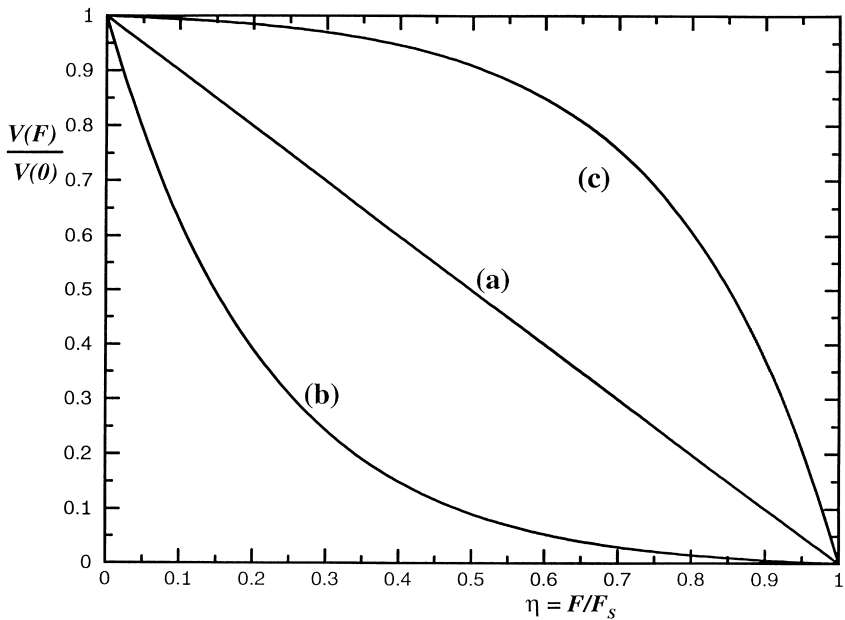


Fig. 3. Examples of nearly linear and of hyperbolic velocity–load plots for $N = 2$ models with rate exponent ε , and reduced transition rate ratios $\bar{w}_j \equiv w_j/u_0$, and load distribution factors $\bar{\theta}_j^\pm \equiv \theta_j^\pm/\theta$, given by the parameter sets $\{\varepsilon; \bar{w}_0 = \bar{w}_1; \bar{\theta}_1^+, \bar{\theta}_0^- = \bar{\theta}_1^-\}$: (a) $\{0.01; 0.99; \frac{1}{2}, 0\}$, (b) $\{9.2; 0.01; \frac{1}{2}, 0\}$, and (c) $\{9.2; 0.01; 0, \frac{1}{2}\}$. Note that $V(0)$ is the velocity at zero load [see (7)] while F_S denotes the stalling load.

For small c the law is close to *linear* [see (a) in Fig. 3] and, in fact, c vanishes whenever

$$u_0 \Delta_1^+ + u_1 \Delta_0^+ = w_0 \Delta_1^- + w_1 \Delta_0^- . \tag{35}$$

This condition has many solutions; for example, if the backward rates are small, so that $\delta \equiv (w_0 + w_1)/(u_0 + u_1) \lesssim 0.1$, say, the load-distribution scheme $\theta_0^+ \simeq \theta_1^+ \approx \frac{1}{2}\theta/(1 + \delta)$ yields a near-vanishing c . Velocity–load plots that are fairly linear have frequently been observed in experiments, particularly on kinesin over quite wide ranges of ATP concentration: see, e.g. [7]. Indeed, if u_0 greatly exceeds u_1 , w_0 , and w_1 , the reduced (V, F) plots become insensitive to u_0 . Then if, as discussed above in Section 2, one has $u_0 \simeq k_0[\text{ATP}]$, the plots will become independent of the ATP concentration [7]. Furthermore, if ε is large but $(\theta_1^+/\theta)\varepsilon \simeq 1$, the (V, F) plots again become close to linear. On the other hand, recent experiments on kinesin [13] have found convex velocity–load plots — resembling (c) in Fig. 3 — at high concentrations: $[\text{ATP}] = 2$ mM.

Although straight, convex, and concave velocity–load plots are readily generated within the $N = 2$ models, other reasonable values of the six parameters:

$$\begin{aligned} \varepsilon, \quad \bar{w}_0 \equiv w_0/u_0, \quad \bar{w}_1 \equiv w_1/u_0, \\ \bar{\theta}_1^+ \equiv \theta_1^+/\theta, \quad \bar{\theta}_0^- \equiv \theta_0^-/\theta, \quad \bar{\theta}_1^- \equiv \theta_1^-/\theta , \end{aligned} \tag{36}$$

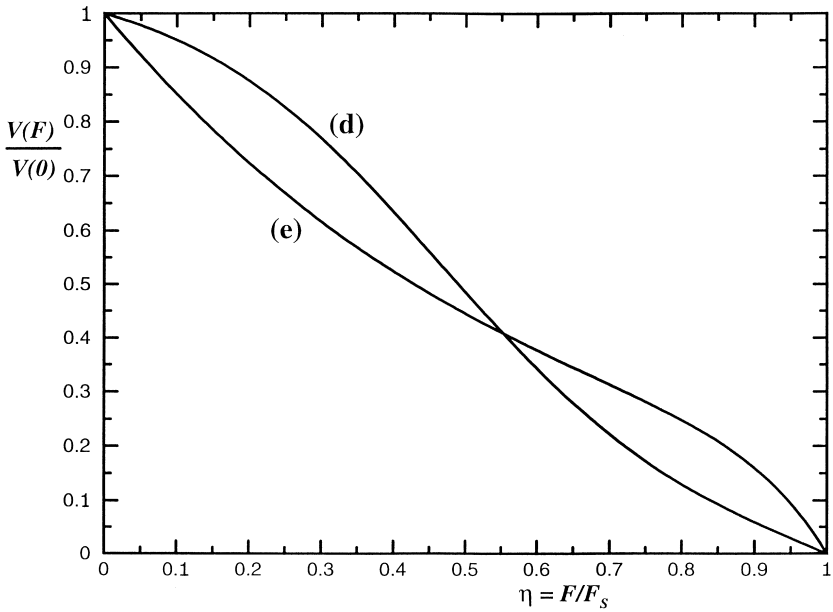


Fig. 4. Velocity-load plots for $N=2$ models displaying points of inflection of opposite sense: the parameter sets are $\{\varepsilon; \bar{w}_0, \bar{w}_1; \bar{\theta}_1^+, \bar{\theta}_0^- = \bar{\theta}_1^-\}$: (d) $\{11.1; 0.15, 10^{-4}; 0, \frac{1}{2}\}$, (e) $\{23.0; 10^{-5}, 10^{-5}; 0.07, 0.43\}$.

yield plots exhibiting points of inflection of either sense, as illustrated in Fig. 4. Plots with a *positive* inflection point, such as (d), have been observed in experiments on RNA-polymerase [12]. However, plots with *negative* inflection points, such as (e), appear to be realized in relatively small regions of the ($N=2$) parameter space. If negative θ_1^+ or θ_0^+ are admitted — as discussed after Eq. (28) — plots with two inflection points are also allowed as example (f) in Fig. 5 demonstrates. Furthermore, in such cases the velocity may even *rise* when a load is initially imposed! See plot (g) in Fig. 5. Thus if one could determine plausible values for the no-load transition-rate ratios, experimental (V, F) plots might, at least within the scope of $N=2$ models, throw some light on the load distribution parameters, θ_j^\pm ; these, we repeat, must be of significance in understanding a motor protein's operation at a molecular level.

7. Relation to Kinesin data

Let us recapitulate briefly: in order to understand the driving force, f , exerted by a molecular motor that takes steps of size d on a molecular track, we have analyzed a broad class of stochastic models: in particular, expressions (2) and (6), embody a general, “linear” motor reaction sequence. In the presence of a constant free-energy source, the motor will achieve a steady velocity $V (> 0)$ but with fluctuations about the mean position, Vt , described by a dispersion or diffusion constant, D , as introduced

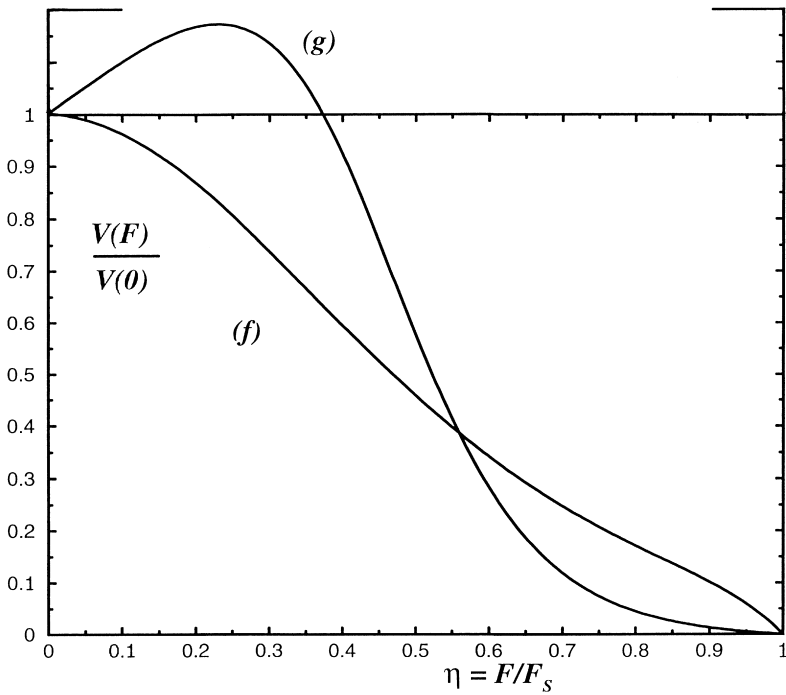


Fig. 5. Further velocity–load plots for $N = 2$ models illustrating a plot, (f), with two (opposite) points of inflection, and one, (g), which is nonmonotonic as well as having a point of inflection: both examples entail one negative load distribution factor, namely, $\theta_1^+ < 0$. The specific parameter values are: $\{\varepsilon; \bar{w}_0, \bar{w}_1; \bar{\theta}_1^+, \bar{\theta}_0^-, \bar{\theta}_1^-\} = \{23.0; 10^{-5}, 10^{-5}; -0.07, 0.48, 0.48\}$, $\{10; 3.4 \times 10^{-4}, 2.5 \times 10^{-3}; -0.1, 0.1, 0.2\}$, respectively.

in (1). Table 1 lists various force scales that have arisen in our analysis and summarizes their relation to the driving force, f . It is useful at this point to attempt to check, at least semiquantitatively, the degree to which our theory for the driving force, the velocity, the dispersion, and their interrelations, satisfactorily corresponds with available experimental data. Because kinesin moving on a microtubule is well studied [1–5, 7–11, 13, 18], it can provide some concrete numerical evidence.⁸

Recall, first, that the microtubule-kinesin step-size, d , is close to 8.2 (or 8.3) nm [10, 13]. In 1994 Svoboda et al. [8] observed a zero-load velocity $V \simeq 670$ nm/s for a concentration $[\text{ATP}] = 2$ mM; in addition, they measured the variance of the motor’s position, $x(t)$, from which we have derived the estimated dispersion $D \simeq 1400$ nm²/s (see also [13]). At $T = 300$ K these results yield the Einstein scale $f_E \simeq 2.0$ pN. On the other hand, the observed stalling force was $f_S \simeq 5\text{--}6$ pN [7, 8]. This is significantly larger than f_E , as we have argued it should be: see Section 4. Note also, by comparing with the maximal force estimate, $f_{\max} \simeq 6.2$ pN [see (13)], that

⁸ Recall footnote 1 regarding Visscher et al. [13].

the observed efficiency \mathcal{E} , is in the range 80–95%. (It may be remarked, however, that this observational estimate of the efficiency does *not* allow for the possible “wastage” of ATP by futile hydrolysis [19] that occurs without translocation of the motor: recall the discussion following (9) in Section 2.)

The “barometric” force scale, f_B , was derived by considering an obstacle that blocks the motor’s motion on the track as illustrated in Fig. 2. The resulting statistically stationary distribution should, quite generally, decay with the distance z from the obstacle like $e^{-\kappa z}$, as asserted in (17). It would, indeed, be interesting and valuable to measure κ and to compare f_B , so derived, with the observed stalling force f_S . It seems likely, however, that such a measurement for kinesin is not currently practicable: indeed, our analysis would suggest a decay length, $\xi \equiv \kappa^{-1}$, of only 0.7 or 0.8 nm.

For the ($N = 2$)-state models on which we have focused (see Section 2), with transition rates u_0 , u_1 , w_0 and w_1 , one has $f_B = (k_B T/d) \ln(u_0 u_1 / w_0 w_1)$. For kinesin (from *Drosophila*) Gilbert and Johnson [18] have studied the kinetics using chemical quench-flow methods. Assuming $[\text{ATP}] = 2$ mM their data show that the values $u_0 = 3800 \text{ s}^{-1}$, $u_1 = 15 \text{ s}^{-1}$, and $w_1 = 200 \text{ s}^{-1}$ represent a sensible map on to an $N = 2$ model; however, the backwards rate from the free state, w_0 , proved unobservably small. Merely for illustration, therefore, let us consider the guess $w_0 = u_1/100 = 0.15 \text{ s}^{-1}$. Via (7) and (8), these rates lead to $V \simeq 116 \text{ nm/s}$ and $D \simeq 474 \text{ nm}^2/\text{s}$, which values yield the Einstein scale $f_E \simeq 1.0 \text{ pN}$ (at $T = 300 \text{ K}$), while the barometric approach gives $f_B \simeq 3.8 \text{ pN}$. The agreement with the estimates based on the results of Svoboda et al. is not so impressive. Nevertheless, the orders of magnitude, the inequality $f_B > f_E$, and the rough equality $f_B \simeq f_S$, are in full accord with our theoretical predictions.

More recently, Higuchi et al. [10] obtained data (for bovine brain kinesin) from which we estimate $u_0 \simeq 1400 \text{ s}^{-1}$ and $u_1 \simeq 45 \text{ s}^{-1}$, in only rough agreement with the values derived from Gilbert and Johnson [18]. The further ad hoc assumption $w_1/u_0 \simeq w_0/u_1 \simeq 1/100$ then yields the values $V \simeq 355 \text{ nm/s}$ and $D \simeq 1370 \text{ nm}^2/\text{s}$ which are rather closer to the observations of Svoboda et al. [7,8]. Likewise, the corresponding values $f_E \simeq 1.1 \text{ pN}$ and $f_B \simeq 4.7 \text{ pN}$, now accord better with the direct experiments (although, of course, depending logarithmically, that is, weakly, on our guesses for w_0 and w_1). We may conclude that, while our general theoretical picture is supported, further experiments (such as [13]) and the use of standardized kinesin samples will certainly be valuable and could provide more stringent tests.

As explained in Section 5, to discuss the velocity $V(F)$ of a motor under a load F , the transition rates in any model must be modified: thus, in our quasiequilibrium hypothesis, (27), the load-distribution factors, θ_j^\pm , recognize that the various transitions in a real motor protein molecule almost certainly accept quite different fractions of the total stress: see also [13]. Indeed, the *acceleration* of some forward rates (corresponding to negative θ_j^+) could provide a mechanism to conserve, e.g., ATP, under “no-load” conditions: recall Fig. 5(g) where $V(F)$, and hence the rate of free-energy consumption, reaches a maximum only under imposition of a load.⁹

⁹ A question conveyed to us from Jonathan Widom stimulated these remarks.

It is natural, as explained, to take the overall load-distribution factor θ in (28) as unity since this leads to the equality of f_S and f_B : compare (21) and (31). However, except for operation close to equilibrium, the hypothesis $\theta = 1$ can be doubted for real motors or more realistic models. It might well be tested by experiment or, probably more feasibly, by simulation.

As seen in (33), the dependence of $V(F)$ on the transition rates and load factors is quite complex even for the simplest two-state models. Indeed, Figs. 3–5 demonstrate that the six independent parameters (36) permit velocity–load plots of extremely varied shapes (including further forms not shown). Although certain types, such as (e), seem to characterize fairly small regions of the parameter space, it seems that, in general, the variation of V with F may reveal comparatively little about the motor mechanism or specific parameter values. Currently, therefore, beyond noting the variety of shapes seen experimentally (as mentioned in Section 6 and note especially [13]), we may say that the observed motility data provide mild support for the concrete aspects of the theory.

Nevertheless, it is worth noting that *negative*, i.e., assisting loads ($F < 0$) are predicted to speed up the motor and this has been observed [11]. Conversely, under super-stalling loads ($F > F_S$), *backwards velocities* are predicted: single reverse steps of kinesin have then been seen [11] which are, thus, *consistent* with our concept of blocked distribution as in (17). However, no steady reverse velocities have been reported. These facts probably reflect the very small terminal reverse rates, w_0 , of kinesin [18] already commented upon. Indeed, we may note, complementing the discussion leading to the Michaelis–Menten relation (5), that these transitions presumably describe second (or higher)-order chemical reactions controlled by the low concentrations of hydrolysis products. The frequently observed process in which a kinesin molecule detaches itself from or “falls off” the track [7,11] should also be included in a fuller account. (Indeed, the exact analysis of Derrida [16] we have used in our discussions, can be generalized to allow for detachment or “death” processes [28].)

The adequacy of the stochastic models encompassed in the kinetic schemes (2)–(4), might be challenged by the existence of *lower bounds* on the dispersion, D , which yield the *upper* bounds on the Einstein scale, f_E , that were mentioned briefly at the end of Section 4. For kinesin at $T = 300$ K the upper bound on f_E is 2.03 pN for any ($N = 2$)-state model. The data of Svoboda et al. [7,8] essentially satisfy this bound; but were the bound violated, one might conclude that a kinetic model with $N = 3$ or more states was needed since the bound increases with N . However, as we demonstrate in the next section, models in which the transitions are described by *discrete jumps* occurring after certain waiting times, are *not* susceptible to these constraints. Such models might well prove more realistic — especially in more complicated molecular motors like RNA polymerase [12] — although, at present, the simpler kinetic representations may suffice. Nevertheless, in assessing our (essentially tentative) comparisons with experiment, it should be borne strongly in mind that the main principles we have enunciated are *not* restricted to the $N = 2$ sequential kinetic models specifically analyzed. Consequently, the observation of significant violations would indicate serious deficiencies

in the general understanding of molecular motor mechanisms embodied in the analysis presented.

8. Jump-and-wait models

As mentioned above, the Einstein force scale, f_E , obtained from the kinetic scheme (2) is subject to a fairly stringent bound. From a more fundamental point of view this can be regarded as arising from a lower bound on the dispersion D for a given velocity V . Since, by (15), $f_E \propto V/D$ this yields an upper bound on the Einstein scale. Specifically, analysis of the explicit expressions (7)–(9) with (6), enables us to establish the bound

$$D \geq Vd/2N \quad (\text{all } u_j, w_j > 0) \quad (37)$$

for $N=2$ kinetic models. The bound is achieved (when $N=2$) by *uniform* rates, that is $u_j = u_0 \gg w_j = w_0$ (all j). This observation can be understood heuristically since in a uniform situation there are no distinguished “rate-limiting steps” in the reaction cycle. For general N , the same uniformity condition yields (37) as an *equality*. Examining numerical examples for small $N \geq 3$, convinces one that, in accord with the heuristic argument, any departure from uniform rates increases D . Thus we believe that inequality (37) is valid for *all* N .¹⁰ (In passing, we may mention that the particular $N=2$ model studied in [15] also respects an *upper* bound on D and, hence, obeys the *lower* bound $f_E/k_B T > 2/d$. However, this is directly attributable to the special limiting situation, $w_0=0$, studied there which, as mentioned initially, cannot be literally true in reality.¹¹)

Now any general lower bound on the dispersion of a molecular motor is open to suspicion since, if the motor were “purely mechanical”, it would move forward, under any fixed load (including $F=0$), at a strictly constant rate exhibiting no variance at all. For such an ideal or ‘clockwork motor’ one would, thus, have $D \equiv 0$. Since highly accurate clocks exist in the animal world — albeit made by humans — one should prefer models that allow the dispersionless, purely mechanical limit to be attained. How closely real molecular motors can or do approach the limit is certainly a matter of interest.

In light of these remarks, our purpose in this section is to demonstrate that the bounds on D and f_E are directly related to the *continuous-time* picture of the rate process that is embodied in the kinetic master equations (3) and (4). In essence, these enforce a minimum value of the dispersion D given a value of V . To see this most directly, consider an ($N=1$)-state model with master equation

$$\frac{\partial P_0}{\partial t}(l, t) = uP_0(l-1, t) + wP_0(l+1, t) - (u+w)P_0(l, t), \quad (38)$$

¹⁰ In terms of the randomness parameter of Svoboda et al. [8] this amounts to the lower bound $r (\equiv 2D/Vd) \geq 1/N$.

¹¹ A similar comment applies to the scheme discussed by Svoboda et al. [8] in their appendix where randomness r is subject to the upper bound $r \leq 1$, which again implies $f_E/k_B T \geq 2/d$.

where, for brevity, we have put $u_0 = u \geq w_0 = w > 0$. Then one finds (say, from the expressions in the appendix) the simple results

$$V = (u - w)d, \quad D = \frac{1}{2}(u + w)d^2. \quad (39)$$

Note, now, the lower bound $D > \frac{1}{2}ud^2$, which is approached when $w/u \rightarrow 0$; in this limit V approaches ud so that (37) is recaptured (for the case $N = 1$). Likewise, the upper bound $f_E/k_B T < 2/d$ (for $N = 1$) follows.

By contrast, consider instead a *discrete* event sequence in which a forward or backward jump is attempted at (mean) time intervals $\Delta t = \tau$ (triggered, one might picture for a molecular motor, by the arrival of individual ATP molecules). If $\check{P}_0(l; n)$ is the probability that the (motor) particle is at site l after n jump attempts, one now has [19,21,31]

$$\check{P}_0(l; n + 1) = p_+ \check{P}_0(l - 1; n) + p_0 \check{P}_0(l; n) + p_- \check{P}_0(l + 1; n), \quad (40)$$

where p_+ and p_- are the probabilities of completing a positive or negative step while $p_0 = 1 - p_+ - p_-$ is the probability of remaining at the same site. If one sets $p_+ = u\tau$ and $p_- = w\tau$, and identifies the time as $t \approx n\tau$, this discrete master equation, reduces to the continuous form (38) in the limit $\tau \rightarrow 0$ [17].

Now the mean displacement $\langle x \rangle_1$ after just one attempt is clearly $(p_+ - p_-)d$. Since, by the assumptions of the model, successive jumps are uncorrelated, one has $\langle x \rangle_n = n\langle x \rangle_1$ so that the mean velocity is

$$V = (p_+ - p_-)d/\tau = (u - w)d. \quad (41)$$

Note that the identifications appropriate for reaching the continuous-time limit yield agreement with the corresponding result (39) for V . Because successive jump attempts are uncorrelated, we can compute D using definition (1) with only a *short* time interval: specifically, we may take $t = \tau$. Thus, from $\langle x^2 \rangle_1 = (p_+ + p_-)d^2$ we obtain

$$\begin{aligned} D &= \frac{1}{2}(d^2/\tau)[p_+ + p_- - (p_+ - p_-)^2] \\ &= \frac{1}{2}[u + w - (u - w)^2\tau]d^2. \end{aligned} \quad (42)$$

To see that D now has no positive lower bound for fixed V , we may either specialize to the case $p_0 = 0$ or consider the limit $p_- (=w\tau) \ll p_+$: then one finds

$$D \propto (d^2/\tau)p_+(1 - p_+) \approx Vd(1 - p_+), \quad (43)$$

which becomes indefinitely small when p_+ approaches unity (while $V \rightarrow d/\tau$). Hence there is no lower bound on D or upper bound on f_E in such a discrete jump model. Indeed, it is intuitively clear that in the limit $p_+ = 1$ (so that $p_0 = p_- = 0$) the particle moves in clockwork manner at speed d/τ with no dispersion.

It is important notice, however, that the barometric formulation can be applied directly to the jump model by introducing a barrier, as before, such that site $L + 1 (> 0)$ cannot be reached. Clearly, this can be accomplished by changing only the master equation (40) for $\check{P}_0(L; n + 1)$ by setting $p_- = 0$ so that $p_0 = 1 - p_+$. With the initial condition $\check{P}_0(l; 0) = \delta_{l0}$, this leads precisely to the previous form, (21), but with $\Gamma = p_+/p_-$.

Furthermore, this jump model result agrees exactly with the continuous-time ($N = 1$) expression $\Gamma = u/w$ when, as above, one puts $p_+ = u\tau$ and $p_- = w\tau$. Beyond that, the ratio $R(\varepsilon) = f_B/f_E$ still obeys (23) but with, in leading order, (ω/σ) replaced by $\frac{1}{2}p_- = (1 - p_0)/2(\Gamma + 1)$. For $\varepsilon > 2$ one must have $\frac{1}{2}p_- < 0.06$ and one finds that when ε increases the ratio $R(\varepsilon)$ varies much as discussed above for the continuous case.

The master equation (40) can be readily extended to periodic N -state jump models, in analogy to the kinetic equations (3) and (4), by introducing forward and backward jump probabilities, p_j^+ and p_j^- with $p_j^0 = 1 - p_j^+ - p_j^-$ (for $j = 0, 1, \dots, N - 1$). The absence of a lower bound on D follows merely by considering the uniform situation, $p_j^+ = p_+$, $p_j^- = p_-$ (all j), which obviously reduces the model to the $N = 1$ case just discussed. The barometric formulation can, equally, be implemented and, again, leads to (21) but now with

$$\Gamma = \prod_{j=0}^{N-1} (p_j^+ / p_j^-). \quad (44)$$

Likewise, in order to account for the effects of a load on the motor particle, the quasiequilibrium hypothesis (27) can be adopted for the spatially dependent jump probabilities $p_j^+(l)$ and $p_j^-(l)$.

8.1. Waiting-time distributions

At a deeper level, however, it is reasonable to object that our arguments for the one-state jump models have more or less tacitly assumed that the jump attempts occur with clockwork regularity at times $n\tau$ whereas, more realistically, there should be some *distribution*, say $\psi(t)$, of *waiting times* between one event and the next. More specifically, after arriving at a site one may suppose that the probability of attempting a jump between subsequent times t and $t + dt$ is $\psi(t)dt$. In that case τ should be identified with the mean time between attempts, defined via

$$\tau = \bar{t} \quad \text{with} \quad \bar{t}^n = \int_0^\infty t^n \psi(t) dt \quad \text{and} \quad \bar{t}^0 = 1. \quad (45)$$

Such a waiting-time model may be studied along the lines of Montroll and Scher [17].¹² Provided $\psi(t)$ decreases sufficiently fast when $t \rightarrow \infty$ that the second moment \bar{t}^2 remains finite, the analysis for V and D can be carried through: it shows again that D is, in general, unbounded below while $f_E \propto V/D$ is unbounded above. Indeed, expression (41) for V remains valid. On the other hand, expression (42) for D is no longer accurate: it must be replaced by the, albeit, similar form

$$\begin{aligned} D &= \frac{1}{2}(d^2/\tau)[p_+ + p_- - (1 - \Theta)(p_+ - p_-)^2] \\ &= \frac{1}{2}[u + w - (1 - \Theta)(u - w)^2\tau]d^2, \end{aligned} \quad (46)$$

¹² A restricted N -state version, with no reverse-reaction transitions (which simplifies the analysis appreciably), was discussed in the appendix of Ref. [8].

the new parameter here, namely,

$$\Theta = (\bar{t}^2 - \bar{t}^2)/\bar{t}^2 \geq 0, \quad (47)$$

is the reduced variance of the waiting time and so measures the relative width or “spread” of the distribution $\psi(t)$. As a conveniently general example, suppose $\psi(t) \propto t^{\nu-1}e^{-\gamma t}$ with $\nu, \gamma > 0$. Then one readily finds¹³ $\tau = \nu/\gamma$ and $\Theta = 1/\nu$. The sharp distribution originally assumed evidently corresponds to the limit $\nu \rightarrow \infty$ and then result (46) reproduces (42). Conversely, for $\nu = 1$, when $\psi(t)$ reduces to the simple exponential or Poisson process form $e^{-t/\tau}$, one has $\Theta = 1$ and the ($N = 1$) kinetic model result (39) is recaptured. Indeed, the full kinetic description becomes valid for exponential waiting distributions.

Finally, once one introduces a waiting-time distribution one would clearly prefer to have *distinct* distributions, say $\psi_j^+(t)$ and $\psi_j^-(t)$, for forward and backward jumps out of states j in a multi-state model (in place of $p_+\psi(t)$ and $p_-\psi(t)$ for the ($N = 1$)-state model described). By extending Derrida’s analysis with the aid of the theorem on generalized master equations due to Landman et al. [35], one can, in fact, handle such a general jump-and-wait model precisely. Thereby we obtain [28] closed-form expressions for V and D that depend only on the low-order moments of $\psi_j^+(t)$ and $\psi_j^-(t)$. Indeed the explicit calculations can be carried further by allowing for finite branching processes, say with waiting-time distributions $\psi_j^\beta(t)$, that lead off the main linear reaction sequence (2). Such branching models may be useful, in particular, for describing RNA-polymerase where individual motors exhibit lengthy “pauses” in their motion on a DNA strand [12]. In addition, at some further cost in calculation, we can [28] include “death processes” with waiting-time distributions, $\psi_j^\delta(t)$: the overall probability of finding a motor particle anywhere on the track then decays in time (ultimately at an exponential rate) but those particles that remain on the track should still be characterized by a drift velocity V and dispersion D . As mentioned, this enables one to include irreversible detachment of a motor from its track as seen, e.g., in kinesin experiments [7,11].

9. Conclusions

We have presented a general theoretical framework for addressing the questions of the driving force, f that a molecular motor protein can exert and the relations of f to the velocity under a load and to the positional dispersion of the motor as it moves along its molecular track. While many of the general concepts advanced should be widely applicable, the detailed analysis has focused on a fairly broad and basic class of discrete-state stochastic models — kinetic descriptions in the simplest instance but extended to jump-and-wait models at a somewhat more elaborate level of description. These models prove amenable to a surprising degree of exact analysis.

¹³ The specific results quoted in Ref. [17], Eqs. (75) for $\nu = \frac{1}{2}$ and 2 are in error. In addition the factor 4 in Eq. (76) should read 2. Dr. Harvey Scher has kindly acknowledged that these corrections are needed.

It proves physically essential to recognize that, although in some sense isothermal and isobaric, the crucial physicochemical operations in a motor protein are highly local and take place intrinsically far from equilibrium. Thus close-to-equilibrium, Einstein-type relations between friction, diffusion, and velocity yield only lower bounds on f ; and, in examples like kinesin on a microtubule, these are too small to use as guides to the value of f by factors of three (or more).

By contrast, a “barometric formulation” in terms of a limiting spatial distribution of a model motor faced with a rigid barrier, provides a simple relation for f , in terms of the intrinsic rate constants, that appears quite consistent with available experimental data (although, that is relatively limited).

The barometric approach agrees, in turn (subject to a rather natural, small proviso), with a more elaborate quasiequilibrium hypothesis for the dependence of the rate constants on imposed loads. It is essential in this connection to recognize that the induced stresses in the motor protein molecule will, in general, cause quite different changes in the various “internal” forward and backward rate processes. As a result, a full specification of even the simplest two-state kinetic model requires six independent parameters. The resulting plots of velocity *vs.* force can be quite varied in shape: see Figs. 3–5. However, even precise experimental knowledge of such motility plots and of the dispersion may not suffice to pin down the model parameters. And, of course, the parameters of even a very successful model may, by their nature, provide comparatively little insight into the detailed molecular mechanisms employed by a real motor protein. Nevertheless, we believe that a systematic and general theoretical approach, such as we have expounded, should play a useful role in analyzing and classifying data, simulations, and more elaborate models.

Acknowledgements

We are indebted to Daniel S. Fisher, David A. Huse, Stanislas Leibler, Michelle D. Wang and Benjamin Widom for valuable comments on our work. Correspondence with Hong Qian and Steven M. Block has been appreciated. The support of the National Science Foundation (under Grant CHE 96-14495) is gratefully acknowledged.

Appendix : General expressions for velocity and dispersion

For a one-dimensional hopping model with N states and arbitrary transition rates u_j and w_j , as introduced in Eqs. (2)–(4), Derrida [16] obtained the exact steady-state behavior. For the drift velocity he found

$$V = V[\{u_j, w_j\}_N] = \frac{d}{R_N} \left(1 - \prod_{j=0}^{N-1} \frac{w_j}{u_j} \right), \quad (\text{A.1})$$

where d is the lattice spacing (or step size) while

$$R_N = \sum_{j=0}^{N-1} r_j, \quad r_j = \frac{1}{u_j} \left(1 + \sum_{k=1}^{N-1} \prod_{i=1}^k \frac{w_{j+i}}{u_{j+i}} \right). \quad (\text{A.2})$$

The expression for the dispersion (or diffusion constant) — defined as in (1) — is more elaborate: it may be written as

$$D = D[\{u_j, w_j\}_N] = \{(VS_N + dU_N)/R_N^2 - \frac{1}{2}(N+2)V\} \frac{d}{N}, \quad (\text{A.3})$$

where the further sums are given by

$$S_N = \sum_{j=0}^{N-1} s_j \sum_{k=0}^{N-1} (k+1)r_{k+j+1}, \quad U_N = \sum_{j=0}^{N-1} u_j r_j s_j, \quad (\text{A.4})$$

while the supplementary coefficients are

$$s_j = \frac{1}{u_j} \left(1 + \sum_{k=1}^{N-1} \prod_{i=1}^k \frac{w_{j+1-i}}{u_{j-i}} \right). \quad (\text{A.5})$$

Derrida's methods will also yield further moments of the steady-state walk distribution; but the expressions become increasingly cumbersome and have not been published to our knowledge.

References

- [1] M.E. Fisher, A.B. Kolomeisky, *Proc. Natl. Acad. Sci. USA* 96 (1999) 6597–6602.
- [2] R.C. Woledge, N.A. Curtin, E. Homsher, *Energetic Aspects of Muscle Contraction*, Academic Press, London, 1985
- [3] L. Stryer, *Biochemistry*, 3rd Edition, W.H. Freeman, San Francisco, 1988, pp. 927–944.
- [4] J. Darnell, H. Lodish, D. Baltimore, *Molecular Cell Biology*, 2nd Edition, Scientific American Books, New York, 1990, pp. 832–835.
- [5] R.H. Abeles, P.A. Frey, W.P. Jencks, *Biochemistry*, Jones and Bartlett, New York, 1992, Chapter 30.
- [6] S. Leibler, *Nature (London)* 370 (1994) 412–413.
- [7] K. Svoboda, S.M. Block, *Cell* 77 (1994) 773–784.
- [8] K. Svoboda, P.P. Mitra, S.M. Block, *Proc. Natl. Acad. Sci. USA* 91 (1994) 11 782–11 786.
- [9] H. Kojima, E. Muto, H. Higuchi, T. Yanagida, *Biophys. J.* 73 (1997) 2012–2022.
- [10] H. Higuchi, E. Muto, Y. Inoue, T. Yanagida, *Proc. Natl. Acad. Sci. USA* 94 (1997) 4395–4400.
- [11] C.M. Coppin, D.W. Pierce, L. Hsu, R.D. Vale, *Proc. Natl. Acad. Sci. USA* 94 (1997) 8539–8544.
- [12] M.D. Wang, M.J. Schnitzer, H. Yin, R. Landick, J. Gelles, S.M. Block, *Science* 282 (1998) 902–907.
- [13] K. Visscher, M.J. Schnitzer, S.M. Block, *Nature (London)* 400 (1999) 184–189.
- [14] H. Qian, *Biophys. Chem.* 67 (1997) 263–267.
- [15] A.B. Kolomeisky, B. Widom, *J. Stat. Phys.* 93 (1998) 633–645.
- [16] B. Derrida, *J. Stat. Phys.* 31 (1983) 433–450.
- [17] E.W. Montroll, H. Scher, *J. Stat. Phys.* 9 (1973) 101–135.
- [18] S.P. Gilbert, K.A. Johnson, *Biochemistry* 33 (1994) 1951–1960.
- [19] S. Leibler, D.A. Huse, *J. Cell Biol.* 121 (1993) 1357–1368.
- [20] T. Duke, S. Leibler, *Biophys. J.* 71 (1996) 1235–1247.
- [21] I. Derényi, T. Vicsek, *Proc. Natl. Acad. Sci. USA* 93 (1996) 6775–6779.
- [22] F. Jülicher, A. Ajdari, J. Prost, *Rev. Mod. Phys.* 69 (1997) 1269–1281.
- [23] F. Jülicher, in: *Transport and Structure in Biophysical and Chemical Phenomena*, eds. S.C. Müller, J. Parisi, W. Zimmerman, *Lecture Notes in Physics*, Springer, Berlin, 1999.

- [24] H. Qian, Phys. Rev. Lett. 81 (1998) 3063–3066.
- [25] A. Parmeggiani, F. Jülicher, A. Ajdari, J. Prost, Phys. Rev. E 60 (1999) 2127.
- [26] G.E. Uhlenbeck, L.S. Ornstein, Phys. Rev. 36 (1930) 823–841.
- [27] S. Chandrasekhar, Rev. Mod. Phys. 15 (1943) 1–89, Chapter II.
- [28] A.B. Kolomeisky, M.E. Fisher, to be published.
- [29] W.F. Sheehan, Physical Chemistry, 2nd Edition Allyn and Bacon, Inc., Boston, 1970, Chapter 9.
- [30] P. Atkins, Physical Chemistry, 6th Edition, W.H. Freeman and Company, New York, 1999, Chapters 4 and 5.
- [31] N.G. van Kampen, Stochastic Processes in Physics and Chemistry, North-Holland, Amsterdam, 1981, Chapters 8, 5, 6.
- [32] M. Doi, S.F. Edwards, The Theory of Polymer Dynamics, Clarendon Press, Oxford, 1986, Chapter 3.
- [33] K. Tawada, K. Sekimoto, J. Theor. Biol. 150 (1991) 193–200.
- [34] L.D. Landau, E.M. Lifshitz, Statistical Physics, 3rd Edition Pergamon Press, London, Part 1, 1980, p. 114.
- [35] U. Landman, E.W. Montroll, M.F. Shlesinger, Proc. Natl. Acad. Sci. USA 74 (1997) 430–433.